Transactions of the Materials Research Society of Japan 28 [4] 1161-1164 (2003)

Ultrathin Au Films with Ultraviolet Transparency and Conductivity Deposited by Dual Ion Beam Sputtering

Satoshi IWATSUBO
Toyama Industrial Technology Center, 383 Takata, Toyama, Toyama 930-0866
Fax: 81-76-433-5466, e-mail: iwatsubo@itc.pref.toyama.jp

Au films were deposited by dual ion beam sputtering. The voltage for Ar ion acceleration V_A was varied in the range between 80 and 800 V. The V_A dependence of the morphology, the resistivity ρ and the transmittance T of the films was investigated. The grain size of the films was smaller and more uniform than that of without Ar bombardment and increased with an increase of V_A. At V_A of 200 V, ρ of the films took the minimum value of 12 μΩcm, and T took the maximum value. Next, the two kinds of Au films, without Ar bombardment [B_{NON}], and with Ar bombardment of 200 eV [B_{DUR}], were deposited as a function of thickness t_F. The t_F dependence of the morphology and properties was investigated. The conductive films in layer structure at t_F above 8 nm for B_{NON} and 2.8 nm for B_{DUR} were deposited, respectively. T for ultraviolet rays of the conductive films was higher than 62 % for B_{NON} and 75 % for B_{DUR}. These results indicate that Ar bombardment can suppress the thickness of initial growth region in island structure and is useful to deposit the conductive ultrathin Au films with high transparency for ultraviolet rays.
Key words: Au, ion beam, sputtering, optical properties, ultrathin film

1. INTRODUCTION

Transparent conductive films, represented by In_2O_3: Sn (ITO) and ZnO are widely used as electrodes for flat panel displays, solar cells and electroluminescence (EL) devices. [1]-[3] ITO has been utilized in various applications and the resistivity has reached 10^{-4} Ωcm as a result of research. However, the band gaps of them are under 4 eV. So, the thick films can not be used for ultraviolet region. Recent technology requires ultraviolet transparency for high density recording and high conversion efficiency. The thick films of $MgIn_2O_4$ [4], $ZnGa_2O_4$ [5] and Ga_2O [6] with the band gap higher than 4 eV were researched. However, their films with a low resistivity nearly equal to ITO films could not be prepared. Therefore, ultrathin metallic films are available instead of such thick conductive films. Then, it is necessary to deposit the films as thin as absorption of ultraviolet rays become negligible.

Au is a typical metal for electrode. So far, Au films deposited by various deposition methods, such as evaporation, ion implantation and so on. Their Au films were almost in separate islands up to the film thickness around 10 nm and nonconductive. [7], [8] For a film growth, surface diffusion and mobility of adatoms during deposition are essential parameters. Especially, their parameters significantly influence film structure during initial growth stage. Ar bombardment by dual ion beam sputtering can control their parameters by collisions between atoms of the films and the Ar ions and modify surface morphology and structure of the films. So, the bombardment with the optimum energy can form very smooth surface. [9] The effect may be useful for suppression of nonconductive island structure during the initial growth stage.

In this study, Au films were deposited by dual ion beam sputtering as a parameter of acceleration voltage for Ar ion V_A. The optimum bombarding energy to deposit the Au films with low resistivity was investigated. So, to be clear the bombarding effect for the initial growth, the two kinds of Au films, without Ar bombardment [B_{NON}] and with Ar bombardment during deposition [B_{DUR}] were deposited. The relationships among the morphology, the electrical and optical properties were investigated as a function of the film thickness t_F.

2. EXPERIMENTAL PROCEDURE

Dual ion beam sputtering apparatus with ion sources of Kaufman type was used in this study. The residual gas pressure in the sputtered-deposition chamber was 6×10^{-5} Pa. Ar gas for sputtering and bombarding was introduced into each ion source at the gas flow rate of 2 sccm. The total pressure was 7.2 mPa. A high purity (99.9%) Au target and water-cooled glass substrates were used. The voltage and the current for the sputtering ion source were set at 1200 V and 30 mA, respectively. The acceleration voltage V_A of the bombarding Ar ions was varied between 80 and 800 V.

Then, the current density of bombarding Ar ions onto the substrate surface was fixed at value of 0.49 A/m^2. Under this condition, the number of Ar ions to bombard the substrate surface is nearly the same as that of the sputtered Au atoms which were estimated on the deposition rate without Ar bombardment. t_F was measured by the calibrated thickness sensor of quartz-crystal resonator. The morphology in the films was observed by TEM. The resistivity ρ was measured using by four terminal method. Concentration and mobility of free electron were estimated from Hall measurements at room temperature by Van del Pauw method. So, the value of t_F was verified by comparison with the film thickness calculated from the concentration. The optical transmission spectra of the films were measured by a spectroscope in the wave range from 200 to 400 nm.

3. RESULTS AND DISCUSSION

3.1 DUAL ION BEAM SPUTTERING

Figure 1 shows the typical TEM images of the Au films deposited by various V_A. The film thickness was 11 nm. V_A of 0 V means the condition without Ar bombardment. The shape and the size of grains were very different between the film at V_A of 0 V and the others. At V_A of 0 V, the large grains of approximate 10 nm in width and the small grains between their large grains were revealed. At V_A of 80 V, the shape of the grains was round. The size of the grains was smaller and more uniform than that at V_A of 0 V. The size increased with an increase of V_A. The gaps through the island grains appeared at V_A above 400 V. The width of the gaps increased as V_A increased.

Figure 2 shows the V_A dependence of the resistivity ρ of the films. ρ gradually decreased at V_A in the range between 80 and 200 V and drastically increased at V_A above 400 V. So, the film was not conductive at V_A of 800 V. ρ took the minimum value of 12 μΩcm at V_A of 200 V before the appearance of the wide gaps between the island grains.

Taking the mean free path of free electron λ_e of the films into the consideration, λ_e is given as following equation. [10]

$$\lambda_e = v_F t_e = \frac{h}{2\pi}\left(3\pi^2 N_e\right)^{\frac{1}{3}} \frac{\mu}{e}, \qquad (1)$$

$$\rho = \frac{1}{\mu e N_e}. \qquad (2)$$

where v_F: electron velocity at Fermi surface, τ_e: electron relaxation time, h: Planck's constant, N_e: electron concentration, μ: electron mobility and e: charge.

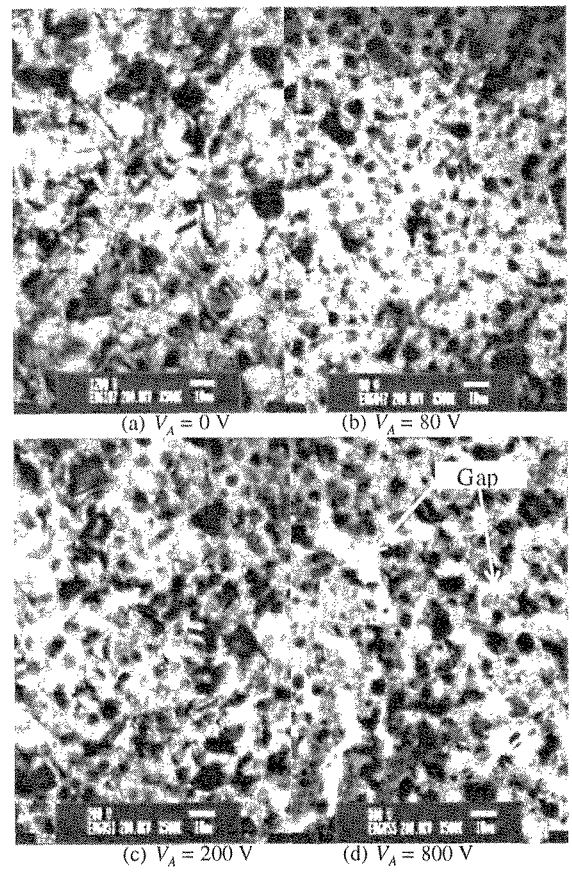

Fig. 1 TEM images of Au films deposited by various V_A.

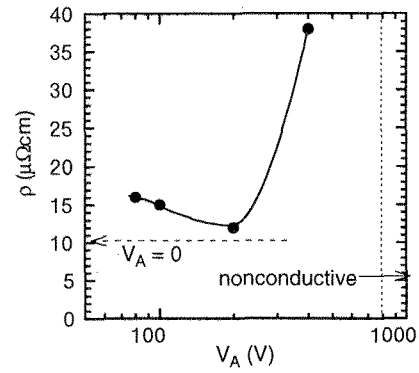

Fig. 2 V_A dependence of resistivity ρ.

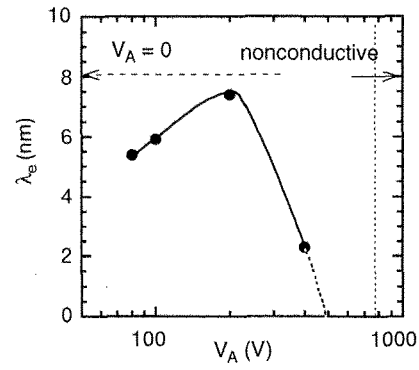

Fig. 3 V_A dependence of mean free path of electron λ_e.

Figure 3 shows the V_A dependence of λ_e of the films. λ_e of the conductive films was in the range between 2 and 7 nm and took the maximum value at V_A of 200 V. These values of λ_e of the films were nearly equal to the average size of the grains of the films. Transmittance T of the film deposited at V_A of 200 V was highest. These results indicate that Ar bombardment is useful to decrease the grain size and to improve the uniformity of the film structure. The effects may lead the increase of T. In addition, the decrease of the grain size may thin down the thickness of island structure during initial growth stage.

3.2 INITIAL GROWTH OF Au FILMS WITH Ar BOMBARDMENT

Next, the two kinds of Au films, without Ar bombardment [B_{NON}], and with Ar bombardment of 200 eV during the deposition [B_{DUR}], were deposited as a function of thickness t_F.

Figure 4 shows the typical TEM images of the Au films deposited by B_{NON} and B_{DUR} as a function of t_F. The images of (a)~(d) and (e)~(h) are for B_{NON} and B_{DUR}, respectively. For B_{NON}, the films with t_F below 2 nm were clearly in separate islands. The films with t_F between 4 and 8 nm were in transitional structure between islands and layer. The films with t_F above 16 nm were completely in layer structure, which combined each island. For B_{DUR}, the films with t_F below 0.7 nm were in separate islands. The films with t_F of 1.4 and 4 nm were in the transitional structure. The films with t_F above 6 nm were completely in layer. The grains of B_{DUR} were smaller than that of B_{NON} at same t_F. The films were conductive at t_F above 8 and 2.8 nm for B_{NON} and B_{DUR}, respectively. These values corresponded with the thickness of the films nearly in layer structure.

Figure 5 shows the structural illustration of the films for B_{NON} and B_{DUR} during the initial growth stage based on the TEM images. The figure indicates that the Ar bombardment can thin down the thickness of island structure of the films owing to the decrease of the grain size and the improvement of the uniformity.

Figure 6 shows the t_F dependence of ρ of the films deposited by various depositions. For reference, ρ of the Au films deposited by conventional RF diode sputtering (RFMS) is also shown. The films of RFMS were conductive at t_F above 10 nm. ρ of the all films gradually decreased with an increase of t_F in the range above 10 nm. The values of ρ, from highest to lowest, were RFMS, B_{DUR} and B_{NON}. At t_F below 10 nm, ρ drastically increased to 10^{-4} Ωcm. It seems that the increase becomes a cause of the size effect owing to electron scattering at interface of films and substrates [11][12], incomplete layer structure and the t_F dependence of the grain size of the films.

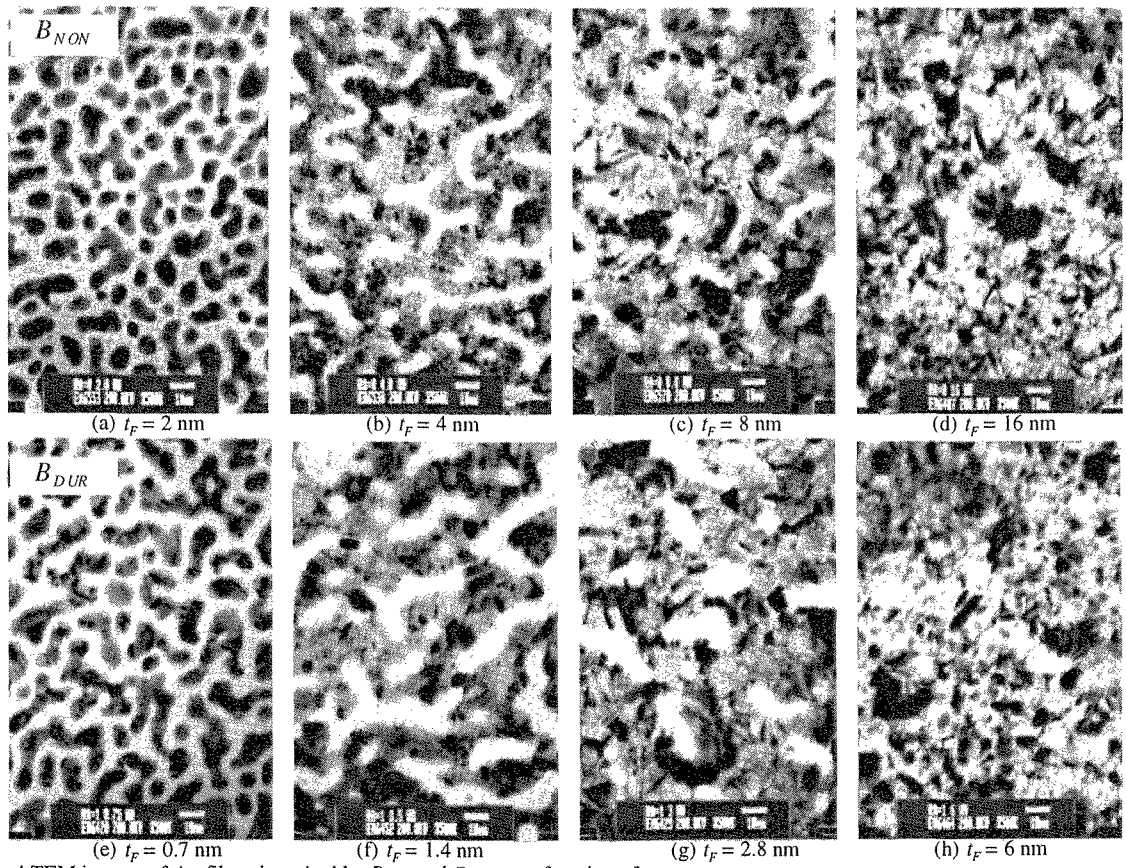

(a) t_F = 2 nm (b) t_F = 4 nm (c) t_F = 8 nm (d) t_F = 16 nm

(e) t_F = 0.7 nm (f) t_F = 1.4 nm (g) t_F = 2.8 nm (h) t_F = 6 nm

Fig. 4 TEM images of Au films deposited by B_{NON} and B_{DUR} as a function of t_F.

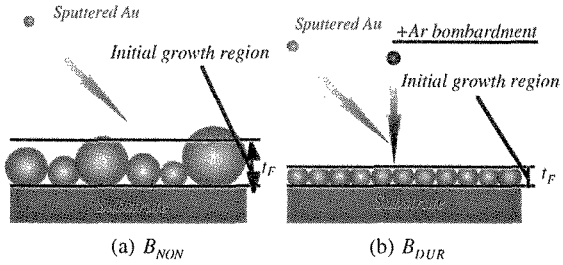

Fig. 5. Structural illustration of Au films deposited by B_{NON} and B_{DUR}.

So, the resistivity of the size effect ρ_{SIZE} was simply estimated as follows. On the assumption that λ_e of the film would not be larger than t_F and from the equations (1) and (2), so that

$$\rho_{SIZE} = \frac{h(3\pi^2)^{\frac{1}{3}}}{2\pi e^2 N_e^{\frac{2}{3}}} \times \frac{1}{t_F} \quad (3)$$

Calculated ρ_{SIZE} is indicated by the broken line in Fig. 6. The values of the experimental ρ are near ρ_{SIZE} at t_F below 10 nm. This result indicates that the size effect can not become negligible for the resistivity of ultrathin films. Therefore, the ultrathin films have an upper limit of ρ_{SIZE}.

Figure 7 shows the T spectra of the conductive Au films. T was higher than 62 % for B_{NON}, 75 % for B_{DUR}, and 56% for RFMS, respectively. The conductive films with high transparency for ultraviolet rays were deposited by the technique using Ar bombardment.

4. CONCLUSION

Au films without and with Ar bombardment were deposited by dual ion beam sputtering. The grain size and the uniformity of the films were very different. The grain size of the films with Ar bombardment was smaller and more uniform than that of the film without Ar bombardment. The grain size increased with an increase of V_A. At V_A of 200 V, ρ took the minimum value of 12 μΩcm and T was maximum.

The conductive films without and with Ar bombardment were at t_F above 8 and 2.8 nm, respectively. T of the conductive films was higher than 62 % for the one and was 75 % for the other. It was found that Ar bombardment can suppress the initial growth in island structure by the effects of the decrease of grain size and the improvement of the uniformity. The technique is useful to deposit the conductive ultrathin Au films with high transparency for ultraviolet rays.

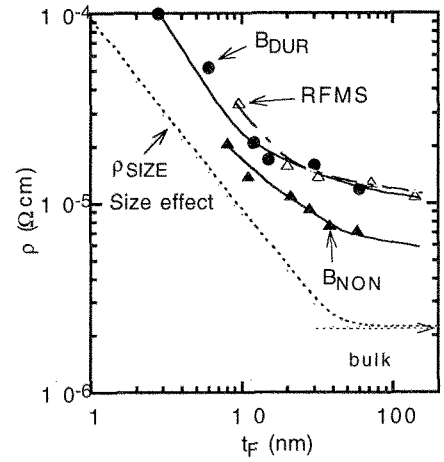

Fig. 6 t_F dependence of ρ of Au films deposited by various depositions.

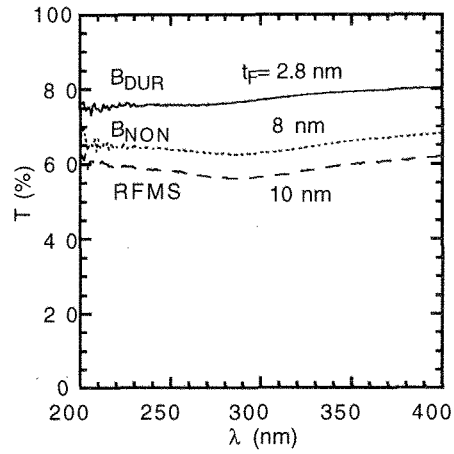

Fig. 7 T spectra of conductive Au films.

References

[1] K. L. Chopra, S. Major and D. K. Pandya, Thin Sold Films, **102**, 1 (1983)
[2] I. Hamberg and C. G. Granqvist, J. Appl. Phys., **60**, R123 (1986)
[3] T. Matsuda, M. Nishino, T. Ohzone and H. Hori, Solod-state Electronics, **41**, 6, 887 (1997)
[4] N. Ueda, T. Omata, N. Hikuma, K. Ueda, H. Mizoguchi, T. Hashimoto and H. Kawazoe, Appl. Phys. Lett., **61**, 1954 (1992)
[5] T. Omata, N. Ueda, N. Hikuma, K. Ueda, H. Mizoguchi, T. Hashimoto and H. Kawazoe, Appl. Phys., **62**, 499 (1993)
[6] N. Ueda, H.Hosono, R. Waseda, H. Kawazoe, Appl. Phys., **70**, 3561 (1997)
[7] E. J. Gillham, J. S. Preston and B. E. Williams, philos. Mag., Ser. 7, **46**, 381 (1955)
[8] L. Holland and G. Siddall, J. Appl. Phys. **9**, 359 (1958)
[9] S. Iwatsubo and M. Naoe, IEEE Trans. Magn., **37**, 2298 (2001)
[10] Kittel, "Introduction to Solid State Physics", John Wiley & Sons, 132-143 (1986)
[11] E. Fuchs, Proc. Cambridge Phil.Soc. **34**, 100 (1938)
[12] E. H. Sondheimer, Phys. Rev. **80**, 401 (1950)

(Received February 5, 2003; Accepted June 30, 2003)